Nuclear Engineering and Technology 49 (2017) 692–699

Available online at ScienceDirect

Nuclear Engineering and Technology

journal homepage: www.elsevier.com/locate/net

Original Article

A Simple Parameterization for the Rising Velocity of Bubbles in a Liquid Pool

Sung Hoon Park [a,*], Changhwan Park [b], JinYong Lee [b], and Byungchul Lee [b]

[a] Department of Environmental Engineering, Sunchon National University, 255 Jungang-ro, Suncheon, Jeonnam 57922, South Korea

[b] FNC Technology, Co., Ltd., 32F Heungdeok IT Valley, 13 Heungdeok 1-ro, Yongin, Gyeonggi 16954, South Korea

ARTICLE INFO

Article history:
Received 28 July 2016
Received in revised form
11 November 2016
Accepted 13 December 2016
Available online 3 January 2017

Keywords:
Bubble Rising Velocity
Bubble Shape
E_o–R_e Plane
Pool Scrubbing
Radioactive Aerosol Emissions

ABSTRACT

The determination of the shape and rising velocity of gas bubbles in a liquid pool is of great importance in analyzing the radioactive aerosol emissions from nuclear power plant accidents in terms of the fission product release rate and the pool scrubbing efficiency of radioactive aerosols. This article suggests a simple parameterization for the gas bubble rising velocity as a function of the volume-equivalent bubble diameter; this parameterization does not require prior knowledge of bubble shape. This is more convenient than previously suggested parameterizations because it is given as a single explicit formula. It is also shown that a bubble shape diagram, which is very similar to the Grace's diagram, can be easily generated using the parameterization suggested in this article. Furthermore, the boundaries among the three bubble shape regimes in the E_o–R_e plane and the condition for the bypass of the spheroidal regime can be delineated directly from the parameterization formula. Therefore, the parameterization suggested in this article appears to be useful not only in easily determining the bubble rising velocity (e.g., in postulated severe accident analysis codes) but also in understanding the trend of bubble shape change due to bubble growth.

1. Introduction

Pool scrubbing has been used in a variety of applications to remove particulate air pollutants, and in particular for removing radioactive aerosols [1–4]. In the pool scrubbing process, aerosol particles are collected on the bubble surface mainly because of gravitational sedimentation, inertial impaction, and Brownian diffusion. The particle removal efficiency of pool scrubbing is dependent on the size, shape, and rising velocity of the bubbles that contain particles.

The shape and rising velocity of bubbles have another significance in the analysis of the emissions of radioactive aerosols in nuclear power plant accidents. A considerable fraction of fission product species contained in radioactive aerosol particles results from product species vaporization from the molten core pool into bubbles formed during the molten core–concrete interaction process [5]. Mass transfer

* Corresponding author.
E-mail address: shpark@sunchon.ac.kr (S.H. Park).
http://dx.doi.org/10.1016/j.net.2016.12.006

between the molten core and the bubbles is highly dependent on the bubble size, shape, and rising velocity. Determination of the bubble shape and rising velocity for a given bubble volume, therefore, is an important procedure in the analysis of radioactive aerosol emissions in terms not only of the pool scrubbing efficiency but also of the fission product release rate. All the postulated severe accident analysis codes currently used worldwide contain their own schemes to determine the bubble shape and rising velocity. The development of an efficient scheme to determine the bubble shape and rising velocity is one of the key issues in enhancing the performance of the accident analysis code in terms of the fission product release.

Several different theories for determining bubble rising velocity are available in the literature [6–13]. Most of those theories deal with a particular bubble shape type, e.g., sphere, spheroid, and spherical (or spheroidal) cap; the bubble shape must be determined in advance to decide which theory to use. The problem, however, is that the bubble shape cannot be determined without information on the bubble rising velocity. This implies that iteration is needed to simultaneously determine both the bubble shape and the rising velocity.

Wallis [14] suggested 10 different bubble rising velocity equations that depend on the size, shape, and rigidity of the bubbles. The study of Jamialahmadi et al [15] was apparently the first effort to suggest a universal formula to determine the bubble rising velocity, but they neglected the effect of inertial force for spherical bubbles. Bozzano and Dente [12] suggested a method to determine the bubble shape and rising velocity simultaneously without iteration. They determined the bubble drag coefficient by assuming that a rising bubble would have such a shape that the total energy (potential energy + surface energy + kinetic energy) is minimized. The results of numerical minimization were approximated into a parameterization, which was a function of two dimensionless parameters: the Eotvos number E_o and the Morton number M. Using the drag coefficient, the bubble rising velocity was given as a solution of a second-order equation.

By analyzing experimental data obtained from 21 different liquids with a very wide range of physical properties, Grace [9] showed that the size, shape, and rising velocity of a single bubble in infinite liquid can be deduced from a diagram in which the relation among three dimensionless numbers, E_o, M, and the Reynolds number R_e, is given graphically. In this diagram (hereafter referred to as Grace's diagram), R_e (representing bubble velocity) was plotted as a function of E_o (representing bubble size) for different values of M (representing liquid properties). Dividing the particle shape into three regimes (sphere, spheroid, and spherical cap), Grace [9] converted the relationships between particle size and rising velocity in the spherical regime (i.e., for small particles) and in the spherical-cap regime (large particles) into relationships between E_o and R_e. Then, for the spheroidal regime (i.e., between those 2 size limits), cross-plotting was used to fill the gap. Grace et al [16] extended the work of Grace [9] to single liquid drops moving in another liquid medium.

Grace's diagram was very useful and provided great insight into the bubble behavior. The boundaries between the spherical and spheroidal regimes, between the spheroidal and spherical-cap regimes, and between the spherical and spherical-cap regimes were visualized in the diagram. Moreover, the condition for the direct conversion of spherical bubbles to spherical-cap bubbles, without passing through the spheroidal regime, was given simply as "$M > \sim 10$." Nevertheless, the determination of R_e using this diagram may be troublesome and liable to error because an interpolation for M is required.

In this article, a simple parameterization that expresses R_e as an explicit function of E_o and M is suggested. This is more convenient than the previously suggested parameterizations because it is given as a single explicit formula. In addition, this parameterization can be used to produce a bubble-shape diagram similar to Grace's diagram.

2. Theories of bubble rising in a liquid pool

Gas bubbles rising in a liquid pool can be categorized based on their shape into one of the following three groups: sphere, spheroid, and spherical cap [10,17]. Bubbles are spherical when they are so small that the inertial force is much smaller than the surface tension or the viscous force. As the bubble size—and hence, the rising velocity—increase, the bubbles change into oblate spheroid shapes because of the resistance imposed by the liquid medium. When the bubbles are sufficiently large, they tend to have flat and often indented bases, breaking the up–down symmetry of the bubble shape. This shape is called the spherical cap.

The shape and rising velocity of a bubble given a volume-equivalent diameter have long been an important subject of fluid mechanics. It is well known that the bubble rising velocity depends on the bubble shape, which in turn is determined according to three dimensionless numbers [9,17]: the Eotvos number $E_o = \frac{g\rho_L d_e^2}{\sigma_L}$, the Reynolds number $R_e = \frac{\rho_L v_b d_e}{\mu_L}$, and the Morton number $M = \frac{g\mu_L^4}{\rho_L \sigma_L^3}$, where g is the gravitational acceleration, ρ_L is the density of the liquid medium, d_e is the volume-equivalent diameter of the bubble, σ_L is the surface tension of the liquid medium, v_b is the terminal rising velocity of the bubble, and μ_L is the viscosity of the liquid medium. E_o is the ratio between body forces and surface tension forces and R_e is the ratio between inertial forces and viscous forces. M, roughly speaking, increases with increasing viscous forces and decreasing surface tension forces.

When the inertial force is negligible compared to the viscous force ($R_e < \sim 1$), the terminal rising velocity of a spherical bubble is given by [6,18]:

$$v_{b,vis} = \frac{g(\rho_L - \rho_G)d_e^2}{6\mu_L}\left(\frac{1+\kappa}{2+3\kappa}\right), \quad (1)$$

where ρ_G is the density of the gas, μ_G is the viscosity of the gas, and $\kappa = \mu_G/\mu_L$. Because for most liquids and gases $\mu_G \ll \mu_L$ ($\kappa \approx 0$) and $\rho_G \ll \rho_L$, Eq. (1) becomes:

$$v_{b,vis} = \frac{g\rho_L d_e^2}{12\mu_L}. \quad (2)$$

Eq. (2) is not valid when R_e is significantly larger than 1 because inertial force is not negligible. Wallis [14] suggested the following formula for spherical bubbles with non-negligible inertial force in an R_e range of $\sim 1 < R_e < \sim 100$:

$$v_{b,in} = 0.14425 g^{5/6} \left(\frac{\rho_L}{\mu_L}\right)^{2/3} d_e^{3/2}. \quad (3)$$

For spheroidal bubbles, v_b is determined by [7,17]:

$$v_{b,spheroid} = \sqrt{\frac{2.14\sigma_L}{\rho_L d_e} + 0.505 g d_e}. \quad (4)$$

For spherical-cap bubbles, the following formula was suggested for v_b [8,17]:

$$v_{b,cap} = 0.721\sqrt{g d_e}. \quad (5)$$

Fig. 1 compares Eqs. (2–5) as a function of d_e. Pure water and air were chosen as the liquid and gas for preparing this figure and the following similar figures in which v_b is plotted against d_e. The rising velocity of a spherical bubble increases with increasing bubble size because increased body force (buoyancy) dominates over increased friction in this shape regime. As the bubble shape changes to spheroid, however, the rising velocity begins to decrease with increasing bubble size because increased friction becomes greater than increased buoyancy owing to the effect of flattening. After the aspect ratio, the ratio of the longer axis length to the shorter axis length, becomes sufficiently large, no further flattening occurs and the rising velocity begins to increase again with increasing bubble size. When the bubbles become too large, the bubbles finally change into the spherical cap shape.

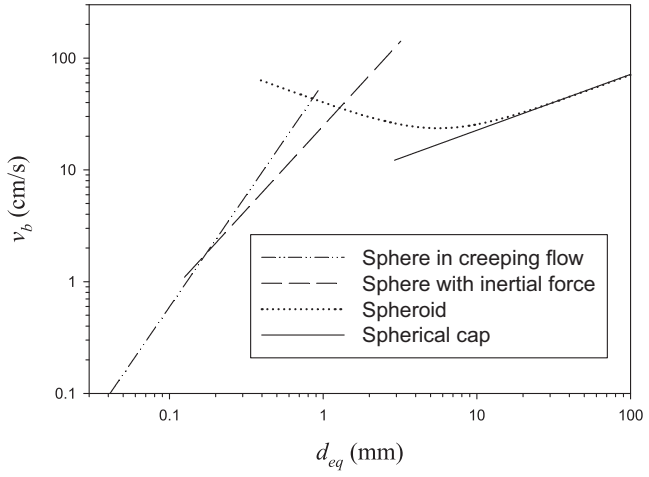

Fig. 1 – Comparison of the bubble rising velocities for three bubble shape regimes: sphere, spheroid, and spherical cap.

3. Parameterization for bubble rising velocity for entire bubble shape range

In this section, a new parameterization that involves all the formulas for the three bubble shape regimes (Eqs. 2–5) is suggested.

The first step is to unify the two regimes for nonspherical bubbles. Fig. 1 shows that Eqs. (4) and (5) exhibit very similar trends for large bubble size. When d_e is sufficiently large ($0.505 g d_e \gg \frac{2.14\sigma_L}{\rho_L d_e}$, i.e., $E_o \gg 4.24$) Eq. (4) converges to

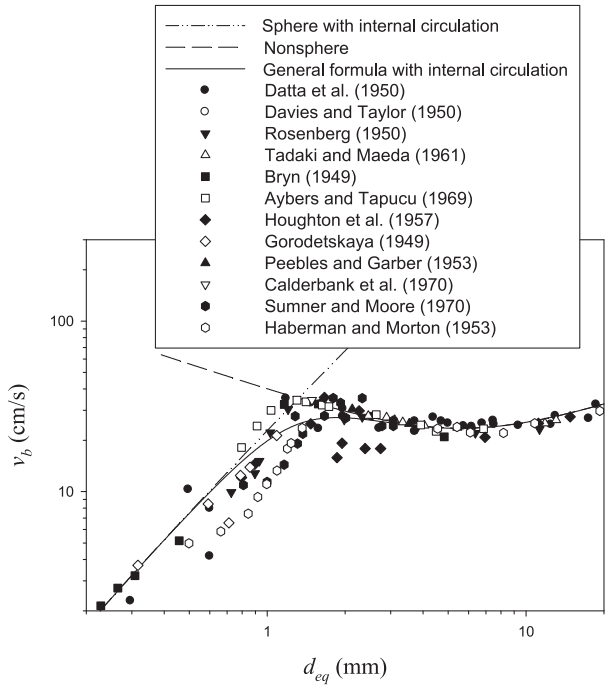

Fig. 2 – General formula for the rising velocity of bubbles with internal circulation compared to experimentally measured data.

$v_b = 0.711\sqrt{g d_e}$, which is almost the same as Eq. (5). Actually, $v_b = 0.711\sqrt{g d_e}$ was suggested for spherical-cap bubbles by Clift et al [17] when $E_o \geq 40$ and $R_e \geq 150$. Therefore, it is suggested to use Eq. (4) not for spheroidal bubbles only but for all nonspherical bubbles.

Second, to let Eq. (2), (3), or (4) be selected automatically for appropriate bubble size and shape, the following equation is suggested for bubbles with arbitrary size and shape.

$$v_b = \min(v_{b,vis},\ v_{b,in},\ v_{b,spheroid}). \quad (6)$$

The reason for using the minimum value in Eq. (6) can be easily seen in Fig. 1. One important advantage of using Eq. (6) is that it is not necessary to identify the bubble shape in advance. Rather, the bubble shape is identified automatically when the bubble rising velocity is determined.

One shortcoming of Eq. (6), however, is that there is an abrupt change in the derivative of the bubble rising velocity when the bubble size–shape regime changes (e.g., from sphere to spheroid). Actually, the transition from sphere to spheroid happens gradually, and the boundary between the two shape regimes is defined somewhat arbitrarily, e.g., by an aspect ratio of about 1.1 [9,10,17], indicating that the abrupt bending at the shape regime boundaries is not natural. Therefore, we suggest the following equation to bridge Eqs. (2), (3), and (4) smoothly:

$$v_b = \frac{1}{\sqrt{\frac{1}{v_{b,vis}^2} + \frac{1}{v_{b,in}^2} + \frac{1}{v_{b,spheroid}^2}}} = \frac{1}{\sqrt{\frac{144\mu_L^2}{g^2\rho_L^2 d_e^4} + \frac{\mu_L^{4/3}}{0.14425^2 g^{5/3}\rho_L^{4/3} d_e^3} + \frac{1}{\frac{2.14\sigma_L}{\rho_L d_e} + 0.505 g d_e}}}. \quad (7)$$

Eq. (7) can be regarded as a combination of the two formulas for spherical and nonspherical bubbles:

$$v_b = \frac{1}{\sqrt{\frac{1}{v_{b,sp}^2} + \frac{1}{v_{b,non-sp}^2}}}, \tag{8}$$

where $v_{b,sp}$ and $v_{b,non-sp}$ are the rising velocities of spherical and nonspherical bubbles, respectively, given by:

$$v_{b,sp} = \frac{1}{\sqrt{\frac{1}{v_{b,vis}^2} + \frac{1}{v_{b,in}^2}}} = \frac{1}{\sqrt{\frac{144\mu_L^2}{g^2\rho_L^2 d_e^4} + \frac{\mu_L^{4/3}}{0.14425^2 g^{5/3}\rho_L^{4/3} d_e^3}}} \tag{9}$$

and $v_{b,non-sp} = v_{b,spheroid}$.

Fig. 2 compares the bubble rising velocity formulas for spherical and nonspherical bubbles with the general formula (Eq. 7) as well as with experimentally measured data [8,10,19–28] reproduced from Clift et al [17]. Despite the general agreement, it is observed that the scatteredness of the data is large and that Eq. (7) tends to overestimate the bubble rising velocity, especially for small bubbles. This can be attributed, at least partly, to the effect of surface contaminants contained in the liquid, which is the subject of the next section.

4. Effects of surface contaminants

Eqs. (2–4) and their combination, Eq. (7), are based on the assumption that internal gas circulation is fully developed when a bubble rises by momentum transfer through the liquid–gas interface. It has often been observed in experiments, however, that small spherical bubbles move with a lower velocity given by the following Stokes equation, which indicates that they behave like rigid bodies with no internal circulation:

$$v_{b,vis} = \frac{g\rho_L d_e^2}{18\mu_L}. \tag{10}$$

The bubble rising velocity predicted by Eq. (10) is 33% lower than that predicted by Eq. (2) because the suppression of gas circulation inside the bubble increases the friction imposed by liquid on the gas bubbles. Frumkin and Levich [13] and Levich and Technica [29] attributed this to the presence of surface-active substances in the liquid medium. According to their explanation, the surface-active substances accumulating at the liquid–gas interface (bubble surface) reduce the surface tension. As the bubbles rise, the surface-active substances are dragged to the bubble bottom, building a surface tension gradient. This gradient creates tangential stress, which suppresses the fluid motion at the interface. The strength of the effect of the surface tension gradient increases with decreasing particle size.

By taking this effect of surface contaminants into account, the rising velocity of spherical bubbles can be expressed by:

$$v_{b,vis} = \frac{1}{f_{sc}} \cdot \frac{g\rho_L d_e^2}{12\mu_L}, \tag{11}$$

where f_{sc} is a factor accounting for the suppressed internal gas circulation due to surface contaminants. The value of f_{sc} is 1.5 when the bubbles are very small and contaminated and hence no internal circulation occurs, whereas it is 1 when the bubbles are not contaminated or are sufficiently large and hence internal circulation fully develops. The value of f_{sc} in real situations varies between 1 and 1.5 depending on the specific contaminants present and their concentrations.

In the same way, the effect of surface contaminants needs to be taken into account also for spherical bubbles with non-negligible inertial force, resulting in the following equation:

$$v_{b,sp} = \frac{1}{\sqrt{\frac{1}{v_{b,vis}^2} + \frac{1}{v_{b,in}^2}}} = \frac{1}{f_{sc}\sqrt{\frac{144\mu_L^2}{g^2\rho_L^2 d_e^4} + \frac{\mu_L^{4/3}}{0.14425^2 g^{5/3}\rho_L^{4/3} d_e^3}}}. \tag{12}$$

Applying this method to Eq. (7), we have:

$$v_b = \frac{1}{\sqrt{\frac{1}{v_{b,sp}^2} + \frac{1}{v_{b,non-sp}^2}}} = \frac{1}{\sqrt{f_{sc}^2\left(\frac{144\mu_L^2}{g^2\rho_L^2 d_e^4} + \frac{\mu_L^{4/3}}{0.14425^2 g^{5/3}\rho_L^{4/3} d_e^3}\right) + \frac{1}{\frac{2.14\sigma_L}{\rho_L d_e} + 0.505 g d_e}}}. \tag{13}$$

The value of f_{sc} must have the following three properties. First, it must be 1.5 for very small bubbles, i.e., for very small E_o. For instance, Bond and Newton [30] argued that internal gas circulation does not occur when $E_o \leq 4$. However, the measurements shown in Fig. 2 indicate that internal gas circulation does not vanish completely for E_o as small as 0.01 ($d_{eq} \approx 0.3\,mm$). Therefore, we assume here that $f_{sc} = 1.5$ for $E_o \leq 0.001$. Second, it must be 1 for very large bubbles. It is assumed here that $f_{sc} = 1$ for $E_o \geq 10$; i.e., bubbles always have internal circulation when body forces dominate over surface tension. Third, it must decrease monotonously with increasing particle size (i.e., with increasing E_o) from 1.5 to 1 in the range of $0.001 \leq E_o \leq 10$. Although several different highly sophisticated methods to determine the value of f_{sc} as a function of E_o were suggested previously [31–33], differences among the methods are relatively large, and their agreements with experimental data are only qualitative. Therefore, a much simpler parameterization for f_{sc} is suggested here:

$$f_{sc} = 1 + \frac{0.5}{1 + \exp\left(\frac{\log E_o + 1}{0.38}\right)}. \tag{14}$$

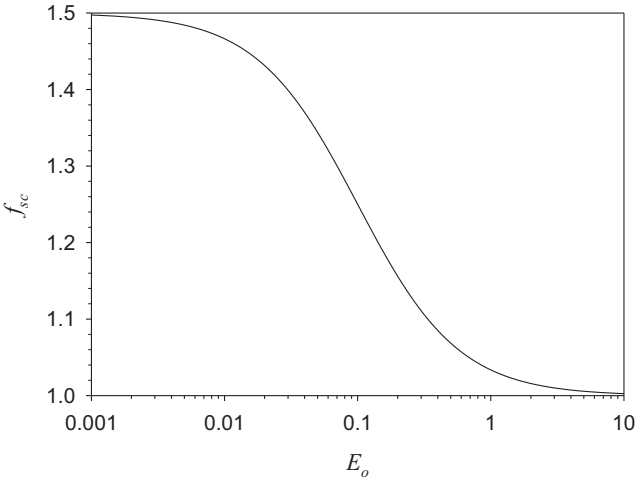

Fig. 3 – Parameterization for f_{sc} as a function of E_o.

The value of f_{sc} calculated using Eq. (14) is plotted as a function of E_o in Fig. 3. It can be clearly seen that Eq. (14) satisfies all the above-mentioned three properties.

Eq. (13) combined with Eq. (14) is the general formula for bubble rising velocity suggested to be approximately valid for any bubble size and shape. Fig. 4 compares it with Eq. (12) (for spherical bubbles), Eq. (4) (for nonspherical bubbles), and Eq. (7) (general formula with $f_{sc} = 1$) as well as with measured data (the same as those shown in Fig. 2) as a function of d_e. For Eq. (12), $f_{sc} = 1$ or 1.5 was assumed depending on whether internal circulation was taken into account. Consideration of the effect of surface contaminants led to better agreement between the parameterization and the measured data obtained with contaminated water (represented by the symbols located lower in the scatter plot), whereas Eq. (7) gives better agreement with the measured data obtained with pure water (represented by the symbols located higher in the scatter plot). Therefore, the scatteredness of the measured data indicates that real systems can fall into various degrees of contamination.

Eq. (13) combined either with $f_{sc} = 1$ or with Eq. (14) can be used for "uncontaminated" and "highly contaminated" liquids, respectively. The bubble rising velocity in "slightly contaminated" liquid may lie between those two limits depending on the degree of contamination. Unfortunately, there is no theory available to represent the factor f_{sc} as a function of the specific contaminants and their concentrations. In practical applications of pool scrubbing, water is inevitably contaminated. In addition, polar liquids are known to be more sensitive to the effect of contamination than nonpolar liquids [17]. Therefore, it is expected that Eq. (13) combined with Eq. (14) can be used in most pool scrubbing applications.

The parameterization suggested in this study is compared with the previous parameterizations found in the literature [12,14,15] in Fig. 5. Except that of Jamialahmadi et al [15], which significantly overestimates the rising velocity of spherical bubbles because it neglects the inertial force, all the

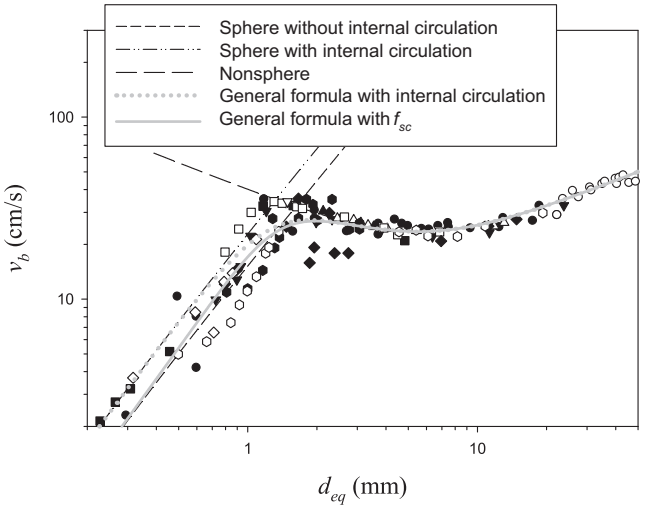

Fig. 4 – Comparison of the general formula [Eq. (13) combined with Eq. (14)] with the formulas for different shape regimes as well as with measured data.

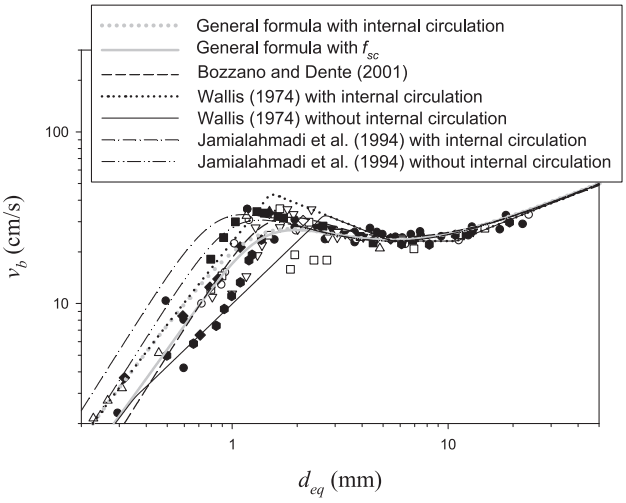

Fig. 5 – Comparison of the parameterization suggested in the present study with previous parameterizations found in the literature.

parameterizations show reasonable agreement with measured data. However, the parameterization in the present study has a couple of distinct advantages over the others. First, it is more convenient than the parameterizations suggested by Wallis [14] and by Bozzano and Dente [12] because it is given as a single explicit formula. Second, it can be used to very easily produce a bubble-shape diagram similar to Grace's diagram that was suggested based on experimental observations (without theoretical justification). This will be the subject of the next section.

5. Discussion

In the work of Grace [9], the boundaries among the spherical, spheroidal, and spherical-cap regimes were delineated in the E_o–R_e plane, in which the bubble size changes for different M values were depicted by parallel lines. Grace's diagram can be produced easily using the results of this study. To do so, it is required to express the equations shown in the previous sections in terms of dimensionless numbers.

By multiplying both sides of Eqs. (12) and (4) by $\rho_L d_e/\mu_L$ and rearranging the equations, the following two equations are obtained for spherical and nonspherical bubbles, respectively:

$$R_e = \frac{1}{f_{sc}\sqrt{\frac{144M}{E_o^3} + \frac{M^{5/6}}{0.14425^2 E_o^{5/2}}}} \quad \text{for spherical bubbles,} \tag{15}$$

$$R_e = \left(\frac{E_o}{M}\right)^{0.25}\sqrt{2.14 + 0.505E_o} \quad \text{for nonspherical bubbles.} \tag{16}$$

Applying the method of bridging two bubble shape regimes to Eqs. (15) and (16), we have:

$$R_e = \frac{1}{\sqrt{f_{sc}^2\left(\frac{144M}{E_o^3} + \frac{M^{5/6}}{0.14425^2 E_o^{5/2}}\right) + \frac{M^{1/2}}{E_o^{1/2}(2.14+0.505E_o)}}}. \tag{17}$$

It should be noted that Eq. (17) can be directly obtained from Eq. (13) by multiplying both sides by $\rho_L d_e/\mu_L$.

In Fig. 6, Eq. (17) is plotted for different values of M ranging from 10^{-14} to 10^{8}. The lines plotted in this figure using Eq. (17) are almost the same as those created by Grace [9]. Besides this, the boundaries between the bubble shape regimes are included in this figure. Detailed discussion of these boundaries is given below.

5.1. Boundary between sphere and spheroid

With the analogy that was used to unify the formulas for bubble rising velocity for spherical and nonspherical bubbles, the boundary between sphere and spheroid can be defined as the point where Eq. (16) (rising velocity of spheroid) begins to be smaller than Eq. (15) (rising velocity of sphere). When R_e is sufficiently large (at the boundary between sphere and spheroid regimes), Eq. (15) converges to:

$$R_e = \frac{0.14425E_o^{5/4}}{f_{sc}M^{5/12}}. \tag{18}$$

Therefore, by equating the right-hand sides of Eqs. (18) and (16), rearranging the resulting equation in terms of M, and combining it with either Eq. (18) or Eq. (16), the following relation between R_e and E_o is obtained.

$$R_e = 7.77f_{sc}^{3/2}\left(1+\frac{4.24}{E_o}\right)^{5/4}. \tag{19}$$

The curve appearing as the boundary between sphere and spheroid in Fig. 6 was plotted using Eq. (19). The sphericity of bubbles increases with decreasing E_o because strong surface tension forces tend to minimize the bubble surface area, and with decreasing R_e because deformation (from spherical shape) is caused by inertial forces and bubbles tend to be spherical under strong viscous forces (relative to inertial forces) [34].

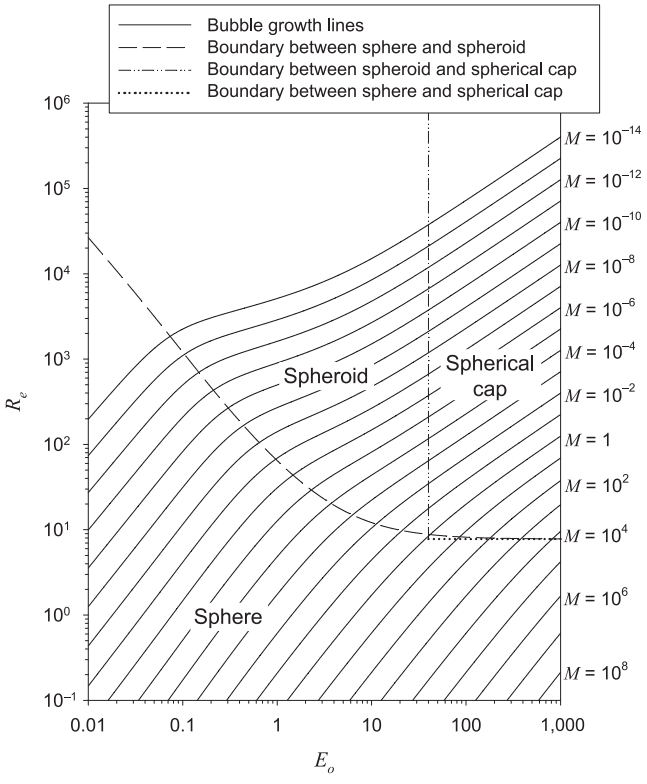

Fig. 6 – Diagram showing different bubble shape regimes in the E_o–R_e plane.

5.2. Boundary between spheroid and spherical cap

In Section 3, Eq. (5) for spherical-cap bubbles was regarded as a limiting case of Eq. (4) (for $E_o \gg 4.24$). The same is obtained from Eq. (16) when the second term in the square root is much larger than the first term. $E_o = 40$ suggested by Grace [9] based on observations agrees very well with the result of this study, where $E_o \gg 4.24$. The boundary between spheroid and spherical cap in Fig. 6 was plotted using $E_o = 40$.

5.3. Boundary between sphere and spherical cap

Considering that the spherical-cap regime can be regarded as a limiting case of the nonspherical regime, with $E_o \gg 4.24$, as mentioned above, the boundary between sphere and spherical cap can be expressed by a limiting case of Eq. (19) with a very large value of E_o, which would result in:

$$R_e = 7.77. \tag{20}$$

This result is somewhat different from that suggested by Grace [9] ($R_e = 1.2$), but the two cases are similar in that the boundary between sphere and spherical cap is given as a constant R_e value (i.e., it does not depend on E_o).

Another important aspect of the boundary between sphere and spherical cap is that it exists only with a value of M larger than a certain value (e.g., ~10, suggested by Grace). When M is smaller than this value, the bubble passes through the spheroid region. This phenomenon can be explained using Fig. 7, in which there are two different cases of the intersection of the rising velocity lines for spherical bubbles and nonspherical bubbles. In the first case (with low M), the rising velocity line for spherical bubbles intersects with that for

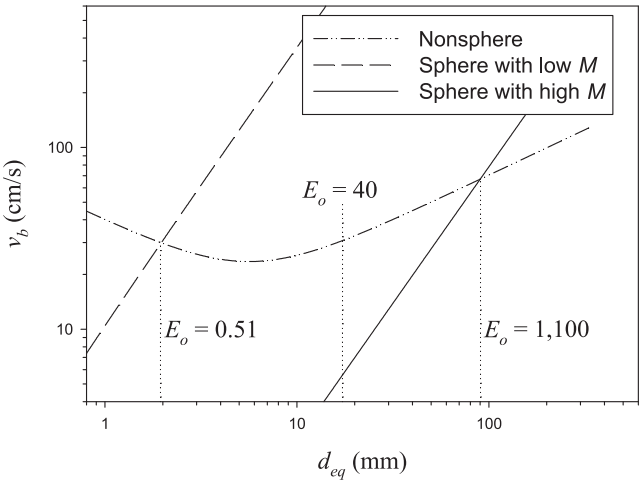

Fig. 7 – Intersection of the rising velocity line for spherical bubbles with low M and high M with that of nonspherical bubbles.

nonspherical bubbles, where E_o is smaller than 40. In this case, the bubble passes through spheroid when it grows. In the second case (with high M), by contrast, the spherical bubble line intersects with the nonspherical bubble line where E_o is larger than 40. In this case, the bubble shape converts directly from sphere to spherical cap. Therefore, whether or not a spheroidal shape appears when a bubble grows can be determined based on the value of E_o at the intersection of the two lines represented by Eqs. (15) and (16). Again, we use Eq. (18) instead of Eq. (15) because the conversion from sphere to nonsphere occurs at $R_e \gg 1$ (see Fig. 5). In addition, f_{sc} can be assumed to be 1 because here we are interested in the phenomenon for E_o of around 40. By equating the right-hand sides of Eqs. (18) and (16), we have:

$$E_o^2 - 24.27M^{1/3}E_o - 102.8M^{1/3} = 0. \quad (21)$$

The solution of Eq. (21) is dependent on the value of M and increases with increasing M. The value of M with which the solution of Eq. (21) is $E_o = 40$ can be found easily to be $M = 3.3$, which is a factor of 3 smaller than the value (~10) estimated graphically from Grace's diagram [9]. It should be noted that the factor of 3 difference is not significant considering that $E_o = 40$ is a rough estimation for the distinction between spheroid and spherical cap.

6. Conclusions

A simple parameterization for the gas bubble rising velocity in a liquid pool was suggested. The parameterization formula was given as an explicit function of the volume-equivalent diameter of a rising bubble. It is not required to identify the bubble shape in advance in using this parameterization to determine the bubble rising velocity.

A bubble-shape diagram, which is very similar to Grace's diagram, was generated using the parameterization suggested in this study. The boundaries among the three bubble shape regimes in the E_o–R_e plane were delineated directly from the parameterization formula: $R_e = 7.77\left(1 + \frac{4.24}{E_o}\right)^{5/4}$ for the boundary between sphere and spheroid; $E_o \gg 4.24$ (practically $E_o = 40$) for the boundary between spheroid and spherical cap; and $R_e = 7.77$ for the boundary between sphere and spherical cap. These formulas for the shape regime boundaries showed good agreement with those suggested by Grace [9] based on experimental observations. Moreover, the condition for bypassing the spheroidal regime (i.e., direct conversion from sphere to spherical cap) was derived from the parameterization and found to be $M \geq 3.3$, which is in order-of-magnitude agreement with that estimated roughly from Grace's diagram ($M \geq \sim 10$). Therefore, the parameterization appears to be useful not only in easily determining the bubble rising velocity (e.g., in postulated severe accident analysis codes) but also in understanding the trend of bubble shape change according to changes in E_o and R_e values due to bubble growth.

Conflicts of interest

All authors have no conflicts of interest to declare.

Acknowledgments

This work was supported by the Nuclear Research & Development of the Korea Institute of Energy Technology and Planning (KETEP) grant funded by the Korea government Ministry of Trade, Industry and Energy (No. 2011T100200045).

REFERENCES

[1] A.T. Wassel, A.F. Mills, D.C. Bugby, R.N. Oehlberg, Analysis of radionuclide retention in water pools, Nucl. Eng. Des. 90 (1985) 87–104.
[2] S.M. Ghiaasiaan, G.F. Yao, A theoretical model for deposition of aerosols in rising spherical bubbles due to diffusion, convection, and inertia, Aerosol Sci. Technol. 26 (1997) 141–153.
[3] C. Gabillet, C. Colin, J. Fabre, Experimental study of bubble injection in a turbulent boundary layer, Int. J. Multiphase Flow 28 (2002) 553–578.
[4] T.S. Laker, S.M. Ghiaasiaan, Monte-Carlo simulation of aerosol transport in rising spherical bubbles with internal circulation, J. Aerosol Sci. 35 (2004) 473–488.
[5] H. Allelein, A. Auvinen, J. Ball, S. Guentay, L.E. Herranz, A. Hidaka, A.V. Jones, M. Kissane, D. Powers, G. Weber, State-of-the-art report on nuclear aerosols, 2009, p. 5. OECD/NEA/CSNI; 2009. Report nr NEA/CSNI/R.
[6] J.S. Hadamard, Mouvement permanent lent d'une sphere liquide et visqueuse dans un liquide visqueux, Comp. Rend. Acad. Sci. 152 (1911) 1735–1738 [in French].
[7] H.D. Mendelson, The prediction of bubble terminal velocities from wave theory, AIChE J. 13 (1967) 250–253.
[8] R.M. Davies, G. Taylor, The mechanics of large bubbles rising through extended liquids and through liquids in tubes, Proc. R. Soc. Lond. Ser. A, Math. Phys. Sci. 200 (1950) 375–390.
[9] J.R. Grace, Shapes and velocities of bubbles rising in infinite liquids, Trans. Inst. Chem. Eng. 51 (1973) 116–120.
[10] T. Tadaki, S. Maeda, On the shape and velocity of single air bubbles rising in various liquids, Kagaku Kogaku 25 (1961) 254–264 [in Japanese].
[11] M. Ishii, N. Zuber, Drag coefficient and relative velocity in bubbly, droplet or particulate flows, AIChE J. 25 (1979) 843–855.
[12] G. Bozzano, M. Dente, Shape and terminal velocity of single bubble motion: a novel approach, Comput. Chem. Eng. 25 (2001) 571–576.
[13] A. Frumkin, V.G. Levich, On surfactants and interfacial motion, Zh. Fiz. Khim. 21 (1947) 1183–1204.
[14] G.B. Wallis, The terminal speed of single drops or bubbles in an infinite medium, Int. J. Multiphase Flow 1 (1974) 491–511.
[15] M. Jamialahmadi, C. Branch, H. Müller-Steinhagen, Terminal bubble rise velocity in liquids, Chem. Eng. Res. Des. 72 (1994) 119–122.
[16] J.R. Grace, T. Wairegi, T.H. Nguyen, Shapes and velocities of single drops and bubbles moving freely through immiscible liquids, Trans. Inst. Chem. Eng. 54 (1976) 167–173.
[17] R. Clift, J.R. Grace, M.E. Weber, Bubbles, Drops, and Particles, Academic Press, New York (NY), 1978.
[18] W. Rybczynski, On the translatory motion of a fluid sphere in a viscous medium, Bull. Int. Acad. Pol. Sci. Lett. Cl. Sci. Math. Nat., Ser. A (1911) 40–46.
[19] R.L. Datta, D.H. Napier, D.M. Newitt, The properties and behaviour of gas bubbles formed at circular orifices, Trans. Inst. Chem. Eng. 28 (1950) 14–26.
[20] W.L. Haberman, R.K. Morton, An experimental investigation of the drag and shape of air bubbles rising in various liquids,

David Taylor Model Basin, Washington (WA), 1953. Report nr DTMB-802.
[21] B. Rosenberg, The drag and shape of air bubbles moving in liquids, David W. Taylor Model Basin, 1950. Report nr 727.
[22] T. Bryn, Speed of rise of air bubbles in liquids, David Taylor Model Basin, 1949. Report nr 132.
[23] N.M. Aybers, A. Tapucu, Studies on the drag and shape of gas bubbles rising through a stagnant liquid, Wärme Stoffübertragung 2 (1969) 171–177.
[24] G. Houghton, P.D. Ritchie, J.A. Thomson, Velocity of rise of air bubbles in sea-water, and their types of motion, Chem. Eng. Sci. 7 (1957) 111–112.
[25] A. Gorodetskaya, The rate of rise of bubbles in water and aqueous solutions at great Reynolds numbers, Russ. J. Phys. Chem. A 23 (1949) 71–78.
[26] F.N. Peebles, H.J. Garber, Studies on the motion of gas bubbles in liquids, Chem. Eng. Prog. 49 (1953) 88–97.
[27] P.H. Calderbank, D.S.L. Johnson, J. Loudon, Mechanics and mass transfer of single bubbles in free rise through some Newtonian and non-Newtonian liquids, Chem. Eng. Sci. 25 (1970) 235–256.
[28] B. Sumner, F.K. Moore, Boundary layer separation on a liquid sphere, National Aeronautics and Space Administration, Washington, D.C, 1970. Report nr NASA CR-1669.
[29] V.G. Levich, S. Technica, Physicochemical Hydrodynamics, Prentice-Hall, Englewood Cliffs, N.J., 1962.
[30] W.N. Bond, D.A. Newton, Bubbles, drops and stokes law, Philos. Mag 5 (1928) 794–800.
[31] P. Savic, Circulation and distortion of liquid drops falling through a viscous medium, National Research Council of Canada, Ottawa, Ontario, Canada, 1953. Report nr MT-22.
[32] R.E. Davis, A. Acrivos, The influence of surfactants on the creeping motion of bubbles, Chem. Eng. Sci. 21 (1966) 681–685.
[33] R.M. Griffith, The effect of surfactants on the terminal velocity of drops and bubbles, Chem. Eng. Sci. 17 (1962) 1057–1070.
[34] T.D. Taylor, A. Acrivos, On the deformation and drag of a falling viscous drop at low Reynolds number, J. Fluid Mech. 18 (1964) 466–476.